U.S. National Library of Medicine
National Center for Biotechnology Information

NLM Citation: Leung K. (*E*)-4-(2-(6-(2-(2-(2-([^{18}F]-fluoroethoxy)ethoxy)ethoxy)pyridin-3-yl)vinyl)-*N*-methylbenzenamine. 2010 Feb 11 [Updated 2010 Dec 9]. In: Molecular Imaging and Contrast Agent Database (MICAD) [Internet]. Bethesda (MD): National Center for Biotechnology Information (US); 2004-2013.
Bookshelf URL: https://www.ncbi.nlm.nih.gov/books/

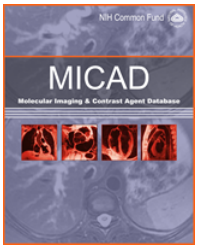

(*E*)-4-(2-(6-(2-(2-(2-([^{18}F]-fluoroethoxy)ethoxy)ethoxy)pyridin-3-yl)vinyl)-*N*-methylbenzenamine

[^{18}F]AV-45

Kam Leung, PhD[1]

Created: February 11, 2010; Updated: December 9, 2010.

Chemical name:	(*E*)-4-(2-(6-(2-(2-(2-([^{18}F]-fluoroethoxy)ethoxy)ethoxy)pyridin-3-yl)vinyl)-*N*-methyl benzenamine
Abbreviated name:	[^{18}F]AV-45
Synonym:	[^{18}F]Florbetapir
Agent category:	Compound
Target:	Amyloid-beta peptide
Target category:	Acceptor
Method of detection:	PET
Source of signal:	^{18}F
Activation:	No
Studies:	• *In vitro* • Rodents • Non-human primates • Humans

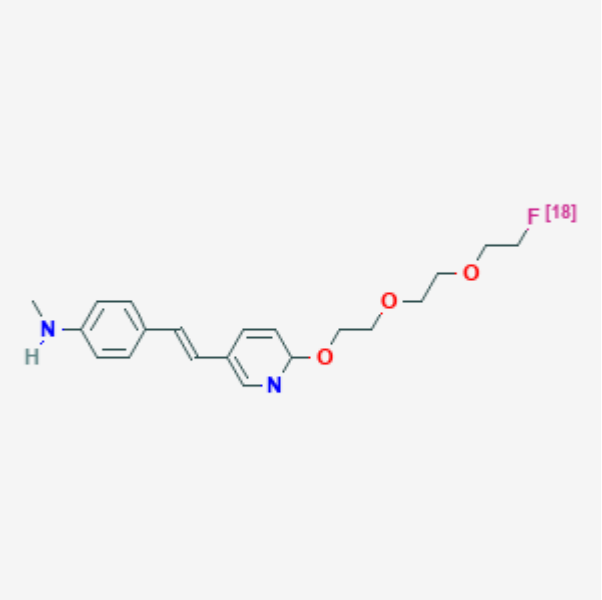

Click on the above structure for additional information in PubChem.

Background

[PubMed]

Alzheimer's disease (AD) is a form of dementia with a gradual memory loss and a progressive decline in mental functions overtime (1, 2). It is characterized pathologically by neuronal loss, extracellular senile plaques (aggregates of amyloid-beta peptides consisting of 40 to 42 amino acids) and intracellular neurofibrillary tangles (filaments of microtubule-binding hyper-phosphorylated protein tau) in the brain, especially in the

Author Affiliation: 1 National Center for Biotechnology Information, NLM, NIH, Bethesda, MD; Email: micad@ncbi.nlm.nih.gov.

hippocampus and associative regions of the cortex (3, 4). β-amyloid peptides and tau protein are implicated as the main causes of neuronal degeneration and cell death (5, 6).

Early diagnosis of AD is important for treatment consideration and disease management (7). Various β-amyloid imaging agents have been developed for magnetic resonance imaging (MRI), single photon emission computed tomography (SPECT), and positron emission tomography (PET) (8-13). The binding of different derivatives of Congo red, thioflavin, stibene, and aminonaphthalene has been studied in human post-mortem brain tissue and in transgenic mice. Out of these analogues, 2-(1-(6-[(2-[^{18}F]fluoroethyl)(methyl)amino]-2-naphthyl)ethylidene)malono nitrile ([^{18}F]FDDNP) was studied in humans, showing more binding in the brains of patients with AD than in those of healthy people (14). However, [^{18}F]FDDNP showed low signal-to-noise ratios for PET imaging, because it is highly lipophilic. *N*-methyl-[^{11}C]-2-(4'-methylaminophenyl)-6-hydroxybenzothiasole, a β-amyloid binding compound based on a series of neutral thioflavin-T derivatives (15), was radiolabeled with the positron-emitting radionuclide ^{11}C ([^{11}C]6-OH-BTA-1 or [^{11}C]PIB). [^{11}C]6-OH-BTA-1 was found to be a promising imaging agent for the senile plaques in the brain (16). Zhang et al. (17) reported the development of a series of fluorinated polyethylene glycol (PEG) units (n = 2-5) for PET imaging of β-amyloid plaques in the brain. Two of them, [^{18}F]{4-[2-(4-{2-(2[2-(2-Fluoro-ethoxy)-ethoxyl]-ethoxy}-phenyl)-vinyl]-phenyl}-methyl-amine ([^{18}F]BAY94-9172, [^{18}F]AV-1) (18) and (*E*)-4-(2-(6-(2-(2-(2-([^{18}F]-fluoroethoxy)ethoxy)ethoxy)pyridin-3-yl)vinyl)-*N*-methyl benzenamine ([^{18}F]AV-45) (19), are being evaluated in clinical trials.

Related Resource Links:

- Chapters in MICAD
- Gene information in NCBI (Amyloid).
- Articles in OMIM
- Clinical trials (Amyloid)
- Drug information in FDA (Amyloid inhibitors)

Synthesis

[PubMed]

[^{18}F]AV-45 was readily synthesized by standard ^{18}F-fluorination of *N*-BOC-protected *O*-tosylated derivative with ([^{18}F]KF/Kryptofix 2.2.2, 120°C for 10 min), followed by hydrolysis (HCl, 120°C for 5 min) (19). The radiochemical yield was 10-30% with the specific activity of 37-185 GBq/mmol (1-5 Ci/mmol) at the end of synthesis. Radiochemical purity was >99% as determined with high-performance liquid chromatography (HPLC). Total synthesis time was not reported.

Yao et al. (20) reported that [^{18}F]AV-45 was prepared in 105 min using a tosylate precursor with Sumitomo modules for radiosynthesis under GMP-compliant conditions. The overall yield was 25.4 ± 7.7% with a HPLC purity of 95.3 ± 2.2% (n = 19). The specific activity of [^{18}F]AV-45 was 470 ± 135 GBq/μmol (12.7 ± 3.6 Ci/μmol, n = 19).

In Vitro Studies: Testing in Cells and Tissues

[PubMed]

[^{18}F]AV-45 has the binding affinity (K_d) value of 3.72 ± 0.3 nM for aggregated β-amyloid fibrils (postmortem AD brain homogenates, n = 4) and the receptor density (B_{max}) value of 8.81 ± 1.64 pmol/mg protein (19). The K_i values for AV-45, PIB, and BAY94-9172 in competition with [^{18}F]AV-45 were found to be 2.87 ± 0.17, 0.87 ± 0.18, and 2.22 ± 0.54 nM, respectively. [^{18}F]AV-45 was bound to the cortex of postmortem AD brain slices but not to control brain slices as visualized by autoradiography studies.

Animal Studies

Rodents

[PubMed]

[18F]AV-45 (0.37 MBq, 10 μCi) was injected intravenously into normal mice (*n* = 3/group) to study its accumulation into the brain and other organs/tissues at 2, 60, 120 and 180 min after injection (19). [18F]AV-45 showed an initial rapid penetration into the brain with 6.23% injected dose (ID)/g at 2 min, with a quick washout (1.84% ID/g at 60 min) in female mice and 7.33% ID/g at 2 min and 1.88% ID/g at 60 min in male mice. The organs with the highest accumulation was the liver (11.07% ID/g) and intestine (12.46% ID/g), followed by the kidney (5.94% ID/g), stomach (4.39% ID/g), and lung (2.58% ID/g) at 60 min after injection. The radioactivity levels were 2.37% and 3.66% in the blood and bone, respectively. The bone radioactivity increased to 7.83% ID/g at 180 min. The rate of defluorination indicated by the bone uptake seems high. There was about 30% intact [18F]AV-45 in the plasma at 30 min after injection with two major metabolites, the *N*-demethylated and *N*-acetylated derivatives of [18F]AV-45. Both metabolites did not show any specific binding to β-amyloid fibrils *in vitro*. *Ex-vivo* autoradiography studies of the brain after injection of [18F]AV-45 in the transgenic Tg2576 mice overexpressing β-amyloid plaques were performed. The brain showed a distinctive labeling of β-amyloid plaques and co-staining with thioflavin-S. No blocking studies were performed.

Other Non-Primate Mammals

[PubMed]

No publication is currently available.

Non-Human Primates

[PubMed]

PET imaging was performed in the brain of one healthy young female rhesus monkey after injection of 174 MBq (4.7 mCi) [18F]AV-45 (19). The radioactivity (4.4% ID) peaked at the cortex at 7 min after injection with quick washout to about the background level of the brain white matter at 20 min.

Human Studies

[PubMed]

Wong et al. (21) used dynamic PET imaging with [18F]AV-45 to study 16 patients with AD and 16 healthy elderly control patients. [18F]AV-45 binding was quantified by use of the standardized uptake value ratio (SUVR), which was calculated for the neocortex, with the cerebellum as reference region. Widespread neocortical binding was observed in all AD patients with a SUVR plateau at 50-60 min after injection with ~370 MBq (10 mCi) [18F]AV-45. A higher neocortical SUVR was observed in AD patients (1.67 ± 0.18) than in healthy controls (1.25 ± 0.18; $P < 0.005$) at 50-60 min. The effective dose was estimated to be 0.013 mSv/MBq (48.1 mrem/mCi). The organs with the greatest exposure were the gallbladder, liver, intestines, and urinary bladder. In a study of three patients with AD and three healthy elderly control patients, Lin et al. (22) reported also a higher SUVR in AD patients (1.51 ± 0.30) than in healthy controls (1.17 ± 0.11) at 50 min after injection with 382 MBq (10.3 mCi) [18F]AV-45.

NIH Support

ROI-AG022559, R43AG032206, K24DA000412, MH078175, AA012839

References

1. Forstl H., Kurz A. *Clinical features of Alzheimer's disease.* . Eur Arch Psychiatry Clin Neurosci. 1999;249(6):288–90. PubMed PMID: 10653284.
2. Heininger K. *A unifying hypothesis of Alzheimer's disease. IV. Causation and sequence of events.* . Rev Neurosci. 2000;11(Spec No):213–328. PubMed PMID: 11065271.
3. Mirra S.S., Heyman A., McKeel D., Sumi S.M., Crain B.J., Brownlee L.M., Vogel F.S., Hughes J.P., van Belle G., Berg L. *The Consortium to Establish a Registry for Alzheimer's Disease (CERAD). Part II. Standardization of the neuropathologic assessment of Alzheimer's disease.* . Neurology. 1991;41(4):479–86. PubMed PMID: 2011243.
4. Hardy J.A., Higgins G.A. *Alzheimer's disease: the amyloid cascade hypothesis.* . Science. 1992;256(5054):184–5. PubMed PMID: 1566067.
5. Hardy J. *The relationship between amyloid and tau.* . J Mol Neurosci. 2003;20(2):203–6. PubMed PMID: 12794314.
6. Brandt R., Hundelt M., Shahani N. *Tau alteration and neuronal degeneration in tauopathies: mechanisms and models.* . Biochim Biophys Acta. 2005;1739(2-3):331–54. PubMed PMID: 15615650.
7. de Leon M.J., DeSanti S., Zinkowski R., Mehta P.D., Pratico D., Segal S., Clark C., Kerkman D., DeBernardis J., Li J., Lair L., Reisberg B., Tsui W., Rusinek H. *MRI and CSF studies in the early diagnosis of Alzheimer's disease.* . J Intern Med. 2004;256(3):205–23. PubMed PMID: 15324364.
8. Bacskai B.J., Klunk W.E., Mathis C.A., Hyman B.T. *Imaging amyloid-beta deposits in vivo.* . J Cereb Blood Flow Metab. 2002;22(9):1035–41. PubMed PMID: 12218409.
9. Nordberg A. *PET imaging of amyloid in Alzheimer's disease.* . Lancet Neurol. 2004;3(9):519–27. PubMed PMID: 15324720.
10. Mathis C.A., Wang Y., Klunk W.E. *Imaging beta-amyloid plaques and neurofibrillary tangles in the aging human brain.* . Curr Pharm Des. 2004;10(13):1469–92. PubMed PMID: 15134570.
11. Klunk W.E., Engler H., Nordberg A., Bacskai B.J., Wang Y., Price J.C., Bergstrom M., Hyman B.T., Langstrom B., Mathis C.A. *Imaging the pathology of Alzheimer's disease: amyloid-imaging with positron emission tomography.* . Neuroimaging Clin N Am. 2003;13(4):781–9. PubMed PMID: 15024961.
12. Wang Y., Klunk W.E., Debnath M.L., Huang G.F., Holt D.P., Shao L., Mathis C.A. *Development of a PET/SPECT agent for amyloid imaging in Alzheimer's disease.* . J Mol Neurosci. 2004;24(1):55–62. PubMed PMID: 15314250.
13. Kung M.P., Hou C., Zhuang Z.P., Skovronsky D., Kung H.F. *Binding of two potential imaging agents targeting amyloid plaques in postmortem brain tissues of patients with Alzheimer's disease.* . Brain Res. 2004;1025(1-2):98–105. PubMed PMID: 15464749.
14. Shoghi-Jadid K., Small G.W., Agdeppa E.D., Kepe V., Ercoli L.M., Siddarth P., Read S., Satyamurthy N., Petric A., Huang S.C., Barrio J.R. *Localization of neurofibrillary tangles and beta-amyloid plaques in the brains of living patients with Alzheimer disease.* . Am J Geriatr Psychiatry. 2002;10(1):24–35. PubMed PMID: 11790632.
15. Bacskai B.J., Hickey G.A., Skoch J., Kajdasz S.T., Wang Y., Huang G.F., Mathis C.A., Klunk W.E., Hyman B.T. *Four-dimensional multiphoton imaging of brain entry, amyloid binding, and clearance of an amyloid-beta ligand in transgenic mice.* . Proc Natl Acad Sci U S A. 2003;100(21):12462–7. PubMed PMID: 14517353.
16. Klunk W.E., Engler H., Nordberg A., Wang Y., Blomqvist G., Holt D.P., Bergstrom M., Savitcheva I., Huang G.F., Estrada S., Ausen B., Debnath M.L., Barletta J., Price J.C., Sandell J., Lopresti B.J., Wall A., Koivisto P., Antoni G., Mathis C.A., Langstrom B. *Imaging brain amyloid in Alzheimer's disease with Pittsburgh Compound-B.* . Ann Neurol. 2004;55(3):306–19. PubMed PMID: 14991808.
17. Zhang W., Oya S., Kung M.P., Hou C., Maier D.L., Kung H.F. *F-18 Polyethyleneglycol stilbenes as PET imaging agents targeting Abeta aggregates in the brain.* . Nucl Med Biol. 2005;32(8):799–809. PubMed PMID: 16253804.

18. O'Keefe G.J., Saunder T.H., Ng S., Ackerman U., Tochon-Danguy H.J., Chan J.G., Gong S., Dyrks T., Lindemann S., Holl G., Dinkelborg L., Villemagne V., Rowe C.C. *Radiation Dosimetry of {beta}-Amyloid Tracers 11C-PiB and 18F-BAY94-9172.* . J Nucl Med. 2009;50(2):309–15. PubMed PMID: 19164222.
19. Choi S.R., Golding G., Zhuang Z., Zhang W., Lim N., Hefti F., Benedum T.E., Kilbourn M.R., Skovronsky D., Kung H.F. *Preclinical properties of 18F-AV-45: a PET agent for Abeta plaques in the brain.* . J Nucl Med. 2009;50(11):1887–94. PubMed PMID: 19837759.
20. Yao C.H., Lin K.J., Weng C.C., Hsiao I.T., Ting Y.S., Yen T.C., Jan T.R., Skovronsky D., Kung M.P., Wey S.P. *GMP-compliant automated synthesis of [(18)F]AV-45 (Florbetapir F 18) for imaging beta-amyloid plaques in human brain.* . Appl Radiat Isot. 2010;68(12):2293–7. PubMed PMID: 20638295.
21. Wong D.F., Rosenberg P.B., Zhou Y., Kumar A., Raymont V., Ravert H.T., Dannals R.F., Nandi A., Brasic J.R., Ye W., Hilton J., Lyketsos C., Kung H.F., Joshi A.D., Skovronsky D.M., Pontecorvo M.J. *In vivo imaging of amyloid deposition in Alzheimer disease using the radioligand 18F-AV-45 (florbetapir [corrected] F 18).* . J Nucl Med. 2010;51(6):913–20. PubMed PMID: 20501908.
22. Lin K.J., Hsu W.C., Hsiao I.T., Wey S.P., Jin L.W., Skovronsky D., Wai Y.Y., Chang H.P., Lo C.W., Yao C.H., Yen T.C., Kung M.P. *Whole-body biodistribution and brain PET imaging with [18F]AV-45, a novel amyloid imaging agent--a pilot study.* . Nucl Med Biol. 2010;37(4):497–508. PubMed PMID: 20447562.